

Continuous random network at the silica surface

V. A. Bakaev*

Department of Chemistry, 152 Davey Laboratory, Penn State University, University Park, Pennsylvania 16802

(Received 18 May 1999)

The continuous random network model for amorphous or liquid silica is proven to be valid for the bulk but the situation at the amorphous silica surface is still unclear. It is shown by molecular-dynamics computer simulation that this model is valid also at the surface of amorphous silica. This was achieved by annealing with a cooling rate inversely proportional to the structural relaxation time. It is shown that the constant of proportionality has an optimum value that minimizes the concentration of nonequilibrium defects.

[S0163-1829(99)05239-X]

The continuous random network (CRN) is a basic model for many amorphous materials like amorphous SiO_2 , Si, Ge, and water.¹ In the case of $\alpha\text{-SiO}_2$, which is only considered in this paper, CRN is a network of corner-sharing SiO_4 tetrahedra without two-member rings (edge-sharing tetrahedra). The validity of the CRN for the bulk atomic structures has been confirmed by many computer simulations and their comparison with experimental studies on liquid and amorphous silica and silicate glasses.²

The question now arises: what is the CRN at the surface? There is no direct experimental information on the radial distribution functions at the surface of amorphous silica. These are main source of information on the atomic structure of the bulk amorphous silica that validate computer simulations.² To circumvent this problem we proposed to use adsorption characteristics of polar molecules like water³ or quadrupolar molecules like carbon dioxide⁴ as a probe of the surface-atomic structure. Computer simulation of adsorption of those molecules on model (simulated) silica surfaces showed that only thoroughly annealed (see below) silica surfaces that has no coordination defects with respect to CRN give simulated adsorption characteristics in agreement with real experiments. On the other hand, adsorption characteristics of simulated amorphous silica surfaces similar to that described in literature, which contain nonbridging oxygens (dangling bonds) at the surface and do not comply with CRN (like, e.g., the silica surface simulated in Ref. 5) deviate considerably from experimental data.

It will be shown below that the surface simulated in Ref. 5 does not correspond to the surface of $\alpha\text{-SiO}_2$, which is formed when liquid SiO_2 solidifies at the glass transition temperature. In what follows, we call such an amorphous surface a solidified liquid surface (SLS). The main problem of the simulation of such a surface is the exceedingly small time scale of molecular-dynamics (MD) computer simulations compared to that of the annealing of real glasses. This is a general problem of glass simulations.⁶ It has been partially overcome here by a nonlinear annealing. The final result of the paper is that the CRN is valid not only for the bulk but also at the SLS.

It should be also emphasized here that SLS is not the only type of amorphous surfaces. Other types are, for instance, fractured surface for which a model⁵ might be a first approximation or the vapor deposited surface as simulated by the *ab initio* MD in Ref. 7.

To simulate SLS, the bulk $\alpha\text{-SiO}_2$ was first simulated by essentially the same method as in Ref. 8: the same *ab initio* potential model was used together with the Ewald summation technique and MD simulation. The number of atoms in a cubic simulation box was 360 with density 2.2 g/cm^3 . The annealing procedure was nearly the same as in Ref. 8 and almost ideal CRN was obtained (see details in Ref. 3). In this simulation, triply periodic boundary conditions (PBCs) in the X, Y, and Z directions were imposed on the simulation box. Then the PBC in the Z direction was removed. The remaining PBC's generate an infinite slab 17.6 \AA (the edge of the cubic simulation box) thick. This slab lies on another slab, which is the copy of the upper one, shifted 1 unit of length down (here and below the unit of length is the edge of the simulation box), the latter lies on the slab shifted 2 units of length down, etc. The highest slab forms surface layer; all the other slabs form substrate.

This is one possible initial state for the $\alpha\text{-SiO}_2$ surface. Other initial states can be generated from the bulk final state by choosing another unit cell (simulation box) in the periodic bulk structure by shifting it along the Z direction by a fraction of its edge. In this way, 10 initial states of the $\alpha\text{-SiO}_2$ surface were generated. These were cross sections of the bulk simulation box on the levels $0.5, 0.4, \dots, -0.4$ where $-0.5 < Z \leq 0.5$. In what follows, a surface simulated by this procedure is called initial surface (IS).

First, the concentration of coordination defects of CRN at each IS was calculated. Coordination defects were determined by the following:³ For each Si atom in the simulation box, the 4 nearest O atoms were determined. Those 4 nearest oxygens constitute the tetrahedron of a Si atom. This tetrahedron may be close to a regular tetrahedron of an ideal CRN or it can be very distorted at the surface (when a Si atom is undercoordinated from the point of view of a stick and ball model). This definition makes Si atoms always 4 coordinated and all coordination defects are transferred to O atoms. The definition is unambiguous because each tetrahedron is unique in the amorphous atomic structure. The oxygen is i coordinated if it is shared by i tetrahedra. If $i=2$ it is a normal bridging oxygen, and the oxygens with other coordinations are coordination defects.

All the O atoms in the simulation box of the surface layer were divided into 6 equal groups (sublayers) in decreasing order of their Z coordinates. The first sublayer is located in

the upper part of the simulation box of about $17.6/6 = 2.9 \text{ \AA}$ thick. Each sublayer is defined to hold 40 atoms but their thickness can vary. The numbers of singly and triply coordinated oxygens in the first sublayer averaged over 10 samples of IS mentioned above was 6.1 ± 0.9 and 4.6 ± 1.0 , correspondingly. In the second sublayer there were practically no (0.1 ± 0.1) singly coordinated oxygens and 4.1 ± 0.8 triply coordinated oxygens. There were practically no singly or triply coordinated oxygens in the other sublayers. No oxygens with coordination other than 1, 2, and 3 were found in these simulations.

The concentrations of singly and triply coordinated oxygens in the first (upper) sublayer was 2.0 ± 0.3 and 1.5 ± 0.3 , respectively per 100 \AA^2 . The concentration of singly and triply coordinated oxygens in the surface layer of $a\text{-SiO}_2$ found in Ref. 5 were 1.9 and 1.53, respectively per 100 \AA^2 at the surface layer 3 \AA thick. These were averages over 12 independent samples of the surface but standard deviations were not indicated.⁵ It is clear, however, that in the limits of the standard deviations given above our data are indistinguishable from those of Ref. 5.

The important difference, however, is that the authors of Ref. 5 had attempted to simulate the annealed $a\text{-SiO}_2$ surface while our data refer to an *unannealed* IS. The explanation of this discrepancy lies with the fact that the simulation of annealing in Ref. 5 was carried out below 1000 K. In computer simulations the glass transition temperature is higher than in real experiments. For SiO_2 it was estimated as 2200 K (experimental value is ca. 1500 K) (Ref. 8). Below this temperature all the essential structural changes in SiO_2 are arrested.^{6,8,9} Thus one might expect that the annealing below 1000 K that was performed in Ref. 5 did not change the number of coordination defects from their values in IS. This was confirmed in our previous paper.⁴

Consider now, the present annealing of IS. First, the level of coordination defects in the equilibrium liquid surface layer was determined in the temperature interval of 3300–4500 K. The interatomic potentials and MD were the same as those used in bulk simulations. However, the Ewald method that is routinely used for computer simulations of bulk silica poses some problems for a surface layer with two-dimensional periodicity. Such a system can be formally considered as triply periodic, one period being infinitely large,¹⁰ however, the method proved to be ineffective for the reasons explained in Ref. 11. There were several attempts to solve the problem (see Ref. 11 and references therein), which give a satisfactory solution for a thin layer. Our surface layer is relatively thick, so we used a conventional trick for such cases: artificially increased the period in the Z direction by two times by adding two empty slabs ($-1 < Z \leq -0.5$ and $0.5 < Z \leq 1$) to the surface layer $-0.5 < Z \leq 0.5$. This trick formally enables one to apply conventional Ewald's method to the surface layer, however, it creates periodic images of the original surface layer, which interact with it. Usually this interaction is neglected. In this paper it was evaluated and corrected by the multipole expansion. Details will be published later because the correction is small and is not essential for the main results of this communication. Thus the system we consider below is the surface layer of 240 O at

TABLE I. Coordination defects in the surface layer of $a\text{-SiO}_2$. The first column—number of a sublayer; N_0 and E (kJ/mol)—parameters of Eq. (1); In N_i^j , i is coordination of oxygen and j designates the state of annealing: $j=0$ —IS; $j=1$ —equilibrium surface coordination layer at 4500 K; $j=2$ —state after slow nonlinear annealing Fig. 3; $j=3$ —state after fast and linear additional annealing to 300 K.

No.	$\ln N_0$	E	N_1^0	N_3^0	N_1^1	N_3^1	N_1^2	N_3^2	N_1^3	N_3^3
1	4.5 ± 0.1	92 ± 4	10	4	4	2	1	0	0	0
2	4.3 ± 0.1	91 ± 4	1	3	3	4	0	0	0	0
3	4.3 ± 0.1	91 ± 4	0	0	6	4	1	3	0	0
4	4.3 ± 0.1	93 ± 4	0	0	4	5	3	0	1	1
5	3.8 ± 0.1	72 ± 3	0	0	3	4	0	2	0	0
6	3.0 ± 0.1	43 ± 3	0	0	4	4	4	2	1	0

oms and 120 Si atoms moving in the external field of the substrate. The substrate atoms are fixed in their initial positions.

The results of these calculations are presented in the second and third columns of Table I. These are coefficients of the relation

$$N = N_0 \exp(-E/T). \quad (1)$$

Here and below, N is the average summary number of singly and triply coordinated oxygens in a sublayer; N_0 and E are coefficients determined by the least square fit of values of $\ln N$ vs $1/T$ in the interval $3300 \leq T \leq 4500$ K. These are equilibrium data (see below). The fact that they reasonably obey Eq. (1) follows from the relatively small standard deviations of the coefficients.

It follows from Eq. (1) that the average number of coordination defects in the first (upper) sublayer at 2200 K (glass transition in the bulk⁸) is 0.6. This is less than 6% of the average summary number of singly and triply coordinated oxygens at IS given above. This suggests that the concentration of coordination defects is negligibly small at the properly annealed $a\text{-SiO}_2$ surface. In what follows, this will be confirmed by direct simulations of SLS.

To this end, one has to evaluate the relaxation time of the coordination defects. In principle this can be done from the time correlation function of the fluctuation of those defects. The power spectrum density (PSD) of those fluctuation is presented in Fig. 1. It was obtained by fast Fourier transform¹² (FFT) of 512 values of N in the first sublayer with a sampling interval $\Delta = 0.16$ ps. The mean arithmetic average was subtracted from the data so that the Fourier coefficient corresponding $n=0$ in Fig. 1 is zero.

PSD is the Fourier transform of the autocorrelation function and makes it possible to estimate the relaxation time of fluctuations τ . If autocorrelation function of N is $C(t/\tau)$, (t is time) then its Fourier transform is $\tau \text{PSD}(\omega\tau)$.¹² The salient feature of PSD in Fig. 1 is the line at $n=2$ corresponding to $\omega = 150$ GHz. The order of magnitude of τ may be estimated from the relation $\omega\tau \sim 1$ that gives $\tau \sim 10$ ps. Since the relaxation time of coordination defects should be close to the structural relaxation time, this is a rough estimate of the structural relaxation time which for a strong liquid like SiO_2 obeys the Arrhenius equation⁶

$$\tau = \tau_0 \exp(E_a/T). \quad (2)$$

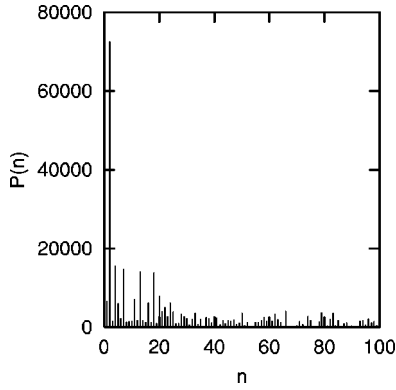


FIG. 1. Power spectral density of the coordination defect fluctuations in the first sublayer at 3500 K. $P(n)=|a_n|^2$, where a_n is the Fourier coefficient of $N(t)$; $0 < t < t_{max}$; $\omega_n = 2\pi n/t_{max}$ and $t_{max} = 82$ ps.

Our data do not give a reliable estimate of the activation energy E_a in this equation. As a first approximation, one can take as E_a the activation energy for diffusion in liquid SiO_2 $E_a = 36\,700 \pm 2100$ K (Ref. 8) since an intrinsic connection between diffusion and structural relaxation is usually assumed.⁶ Now substitute in Eq. (2) $\tau = 10$ ps, $E_a = 38000$ K, and $T = 3500$ K to estimate $\tau_0 \sim 0.1$ fs. With these parameters Eq. (2) gives $\tau = 3$ ns for $T = 2200$ K, which seems reasonable for the glass transition temperature⁸ with the time scale below 1 ns. At $T = 4500$ K, $\tau = 0.5$ ps. With such a small τ , equilibrium is easy to reach in MD simulations.

There is a long stretch of white noise spectrum in Fig. 1. These are lines with $n > 20$ (the interval $100 < n \leq 256$ looks similar to $20 < n \leq 100$ and is not shown in Fig. 1 as well as PSD for the negative values of n). This part of the PSD corresponds to fast fluctuations of N . It has been found that these fluctuations approximately obey the relation

$$\langle (\Delta N)^2 \rangle \approx N \quad (3)$$

and do not explicitly depend on temperature, similar to the fluctuations of point defects (lattice vacancies) in crystals.¹³

Similar spectra of fast fluctuations that do not depend on temperature and much slower fluctuations corresponding to structural relaxation of stress (α process) were observed in computer simulations (see, e.g. Refs. 9 and 14). In analogy with that and other similar results, it is assumed here that the low-frequency part of the power spectral density in Fig. 1 corresponds to the slow relaxation of coordination defects (structural relaxation).

Now, we can discuss in a semiquantitative way the dependence of N on temperature in the process of annealing by cooling liquid SiO_2 starting from some maximal temperature T_0 . Take the simplest relaxation equation

$$\frac{dN}{dT} = \frac{N - N_{eq}(T)}{\Delta T(T)}; \quad \Delta T(T) = -\tau(T) \frac{dT}{dt}; \quad N(T_0) = N_0 \quad (4)$$

(in what follows, $dT/dt < 0$ and $\Delta T > 0$); $N_{eq}(T)$ is given by Eq. (1) and $\tau(T)$ is given by Eq. (2). Let $\Delta T(T) = a$ where a is constant. This fixes the temperature profile $T(t)$ by the differential equation

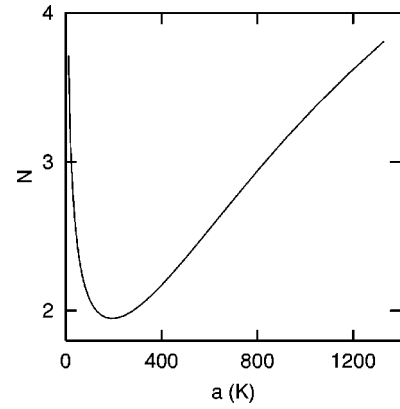


FIG. 2. The final number of coordination defects in the surface layer vs. rate of annealing. Time of annealing is 100 ps; a -parameter in Eq. (5).

$$adt = -\tau(T)dT; \quad T(0) = T_0. \quad (5)$$

In computer simulation the total time of annealing is usually fixed. Thus the final minimal temperature obtained by the solution of Eq. (5) $T = T(a)$ as well as the final (minimal) value of $N = N(a)$ depends only on a . One finds

$$N(a) = N_0 \exp\left[-\frac{T_0 - T(a)}{a}\right] + \int_{T(a)}^{T_0} dT' \frac{N_{eq}(T')}{a} \times \exp\left[-\frac{T' - T(a)}{a}\right]. \quad (6)$$

This function is presented in Fig. 2. It passes through a minimum. This is because on one hand, a larger parameter a in Eq. (5) makes cooling faster and the final temperature $T(a)$ lower. Thus, equilibrium values of N as given by Eq. (1) become lower. On the other hand, faster cooling increases the gap between nonequilibrium values of N (presented in Fig. 2) and the equilibrium ones.

The value of $a = 200$ K that gives minimum N in Fig. 2 corresponds to the temperature profile of annealing shown in Fig. 3. It is strongly nonlinear in contrast to those of Refs. 5 and 8, which were partially linear or stepwise. The time dependence of N in the process of annealing is shown in Fig. 4. One can see the fast fluctuations of coordination defects that produce white noise in Fig. 1. The variance of those fluctuations decreases as the value of N decreases, in line with Eq.

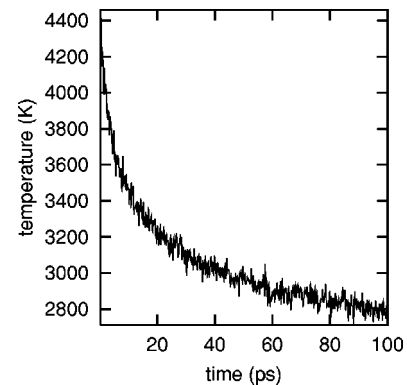


FIG. 3. Temperature profile of annealing.

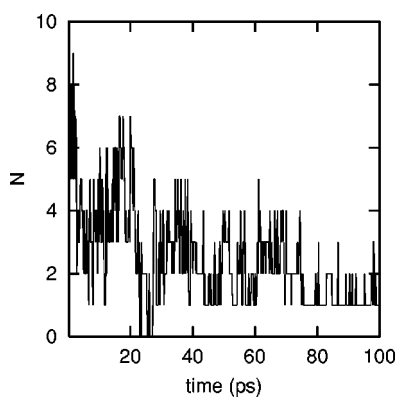


FIG. 4. Coordination defects in the first sublayer (upper part of surface layer) in the process of annealing.

(3). It is seen that coordination defects can disappear from the surface even at high temperature (3200 K) as a result of those fluctuations. However, in average, the level of those defects steadily decreases and is almost constant during the last 20 ps of annealing. Due to the fast fluctuations, the number of coordination defects in the final configuration fluctuates too.

The characteristics of the final configurations in the course of the annealing described by Figs. 3 and 4 are presented in Table I. The N_1^0 and N_3^0 columns show that coordination defects are concentrated at the upper part of IS. The next two columns represent the distribution of coordination defects over the surface layer heated to 4500 K. This is an equilibrium configuration and correspondingly the coordination defects are homogeneously distributed (apart from fluctuations) over the surface layer. N_1^2 and N_3^2 represent coordination defects after annealing shown in Figs. 3 and 4. One may see that coordination defects have almost disappeared from the upper part of the surface layer. Finally, N_1^3 and N_3^3 represent coordination defects in the surface layer after additional annealing with a linear temperature profile from the

lowest temperature in Fig. 4 to 300 K for 50 ps.

The last two columns of Table I represent the final state of the annealed surface layer of a -SiO₂. The three upper sublayers have no coordination defects at all. It was checked that they have also no two-membered rings. Thus coordination of this surface conforms completely with the CRN model.

At the bottom of the surface layer coordination defects are still present after annealing as expected using the values of the parameters of Eq. (1). At 2800 K (the minimal temperature in Fig. 3), Eq. (1) gives $N=1.7$ for the first sublayer and $N=3.2$ for the last (lowest) one. The difference may be due to the interface between the surface layer and the substrate. This could be an artifact of our model but the results for the upper layer seem to be reliable because it is relatively far from that interface. They represent SLS—the surface of a -SiO₂ in the sense determined in the beginning of this communication.

The results presented in the last eight columns of Table I refer to only one computer experiment on simulation of annealing. The values of N_i^j may fluctuate as seen from comparison of N_i^0 with the average values given above. The final values of N_i^3 can fluctuate too so that one might suspect them to be accidental. However, the simulation was repeated three times starting from different IS's and the final results were essentially the same.

In conclusion, it is shown that the CRN that is successful description for bulk is valid also at SLS. This result was obtained by simulation of a nonlinear annealing with cooling rate inversely proportional to the structural relaxation time of amorphous material. The structural relaxation time of coordination defects fluctuations was evaluated (for the first time). It is shown that there is an optimal value for the constant of proportionality determining the cooling rate that minimizes the concentration of nonequilibrium defects in the material at a given total time of annealing.

This work was supported by the National Science Foundation through Grant No. DMR-9803884.

*Electronic address: vab@chem.psu.edu

¹J. M. Ziman, *Models of Disorder. The Theoretical Physics of Homogeneously Disordered Systems* (Cambridge University Press, Cambridge, 1979).

²P. H. Poole, P. F. McMillan, and G. H. Wolf, in *Structure, Dynamics, and Properties of Silicate Melts*, edited by J. F. Stebbins, P. F. McMillan, and D. B. Dingwell, *Reviews in Mineralogy*, Vol. 32 (Mineralog. Soc. Amer., Washington, D.C., 1995).

³V. A. Bakaev and W. A. Steele (unpublished).

⁴V. Bakaev, W. Steele, T. Bakaeva, and C. Pantano, *J. Chem. Phys.* (to be published).

⁵B. P. Feuston and S. H. Garofalini, *J. Chem. Phys.* **91**, 564 (1989).

⁶C. A. Angell, *Science* **267**, 1924 (1995).

⁷J. Dong and D. A. Drabold, *Phys. Rev. B* **57**, 15 591 (1998).

⁸R. G. Della Valle and H. C. Andersen, *J. Chem. Phys.* **97**, 2682 (1992).

⁹L. Angelani, G. Parisi, G. Ruocco, and G. Villiani, *Phys. Rev. Lett.* **81**, 4648 (1998).

¹⁰D. E. Parry, *Surf. Sci.* **49**, 433 (1975); **54**, 195 (1976).

¹¹J. Hautman, M. L. Klein, *Mol. Phys.* **75**, 379 (1992).

¹²W. H. Press, S. A. Teukolsky, W. T. Vetterling, and B. P. Flannery, *Numerical Recipes in FORTRAN* (Cambridge University Press, Cambridge, 1992).

¹³C. Kittel, *Introduction to Solid State Physics* (Wiley, New York, 1956).

¹⁴D. A. Drabold, P. A. Fedders, S. Klemm, and O. F. Sankey, *Phys. Rev. Lett.* **67**, 2179 (1991).